A Copper Rotor Induction Motor Solution for Electrical Vehicles Traction System

Mircea Popescu
Motor Design Ltd.
Wrexham, U.K.
orcid.org/0000-0002-1883-7891

Nicolas Riviere
Motor Design Ltd.
Wrexham, U.K.
nicolas.riviere@motor-design.com

Giuseppe Volpe
Motor Design Ltd.
Wrexha, U.K.
giuseppe.volpe@motor-design.com

Marco Villani
University of L'Aquila
L'Aquila, Italy
marco.villani@univaq.it

Giuseppe Fabri
University of L'Aquila
L'Aquila, Italy
giuseppe.fabri@univaq.it

Lino di Leonardo
University of L'Aquila
L'Aquila, Italy
lino.dileonardo@univaq.it

***Abstract*— This paper deals with the design of a scalable 200kW/ 370Nm or 75kW/ 200Nm, induction machines for electrical vehicles traction system. Two configurations are considered as low cost rare-earth free magnet electric motor alternatives: inner rotor and outer rotor. Both designs allow mass production while providing higher performance compared to current technologies. The electromagnetic, thermal and mechanical constraints are considered throughout the machine design, from the specifications to the optimization. Rotor die-casting, oil spray cooling and hairpin stator winding are used in the analyzed solutions. Analytical and numerical methods are used for electromagnetic and continuous thermal performance calculation over the full speed range of the machine, along with the mechanical limits from a stress and modal point of view.**

Keywords—electrical vehicles, traction motors, induction motors, copper rotor

I. Introduction

The Electrical Vehicles' (EVs) market has kept growing for the last decade, due to new environmental restrictions made by governments in order to reduce gas emissions and to prepare the ecological transition towards the fossil fuel independency. Compared to conventional combustion engines, the electric motors benefit of higher efficiency, braking recovery and provides a noise free solution with a smoother driving, bettering passengers and pedestrians comfort. To limit the global energy consumption and ensure a modular integration into the vehicle, the market demand tends towards more efficient, lighter and more compact motors.

The present study focuses on the development of next generation electric powertrain, avoiding the use of magnets and ensuring the industrial feasibility for mass production at low manufacturing costs. The Induction Machine (IM) is therefore considered a potential candidate. The specifications are reported in Table I. The Key Performance Indicators (KPIs), including efficiency, specific torque, specific power and power density are defined based on Tesla 60s motor [1]. Additional boundary conditions are set based on vehicle requirements, considering the Jaguar XJMY21 as a target.

II. Machine Topology

Even if induction machines present a lower efficiency and torque density than PM motors, the technology is well established in the automotive industry (e.g. Tesla Motors) and it still represents an attractive and feasible solution for EVs, due to its simplicity, robustness, versatility, cost-effective manufacturing aspects and fault tolerant capability.

Horizon 2020, GV04 program, Grant 770143.

TABLE I. Motor Specifications

Requirement	Unit	Value
Peak power	kW	200
Peak torque	Nm	371
Maximum speed	rpm	22000
Nominal torque	Nm	152
Nominal power	kW	70
Peak specific power	kW/kg	4.3*
Peak specific torque	Nm/kg	8.2*
Peak power density	kW/l	8*
Efficiency	%	≥ 94
Maximum DC bus voltage	V	720
Maximum phase current	Arms	500
Maximum dimensions	mm	250 × 250 X 310

In addition, the IM does not use rare-earth materials, ensuring mass production feasibility at lower cost [2]. The copper is usually preferred to the aluminium due to its higher electrical conductivity, higher mechanical strength and better thermal properties. The rotor can be either die-casted or fabricated and both methods are now industry proven [3].

A hairpin winding is used on the stator side. The proposed designs for the IM use exceptional performance of the proprietary hairpin stator winding**.** In contrast to conventional round wire windings, the hairpin stator winding uses precision-formed rectangular wires. Multiple layers of interlocking "hairpins" produce a superior slot fill (up to 73% vs. 40% for typical round-wire windings) [4], [7]. From a thermal perspective, the machine will be stator and rotor cooled and two different solutions are investigated. The first one consists of conventional housing water jacket coupled with a spiral groove shaft cooling system, using a mixture of ethylene, water and glycol mixture as a coolant. The second one is equipped with a spray cooling system with nozzles places on the housing jacket and the hollow shaft surface, cooled by automatic transmission fluid.

The adopted designs are outlined in Fig. 1. A copper rotor induction motor (CR-IM) topology is employed: stator with 36 slots and rotor with 50 bars topology are used for both (a) inner and (b) outer rotor configurations. The number of magnetic poles is different for two configurations: 4-pole for inner rotor, and 6-pole for outer rotor respectively.

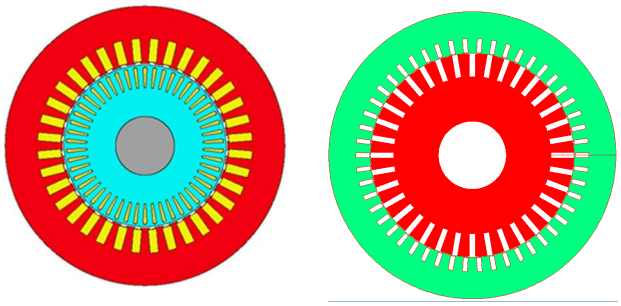

(a) (b)

Fig. 1. Radial and axial cross sections of proposed induction motor designs: a) inner rotor; b) outer rotor.

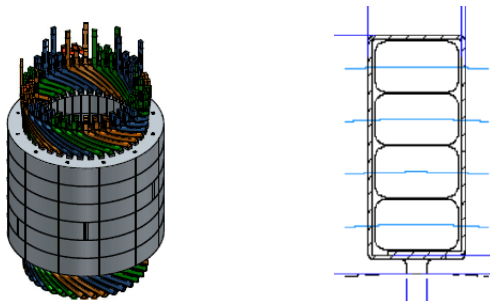

(a) (b)

Fig. 2. Hairpin winding (a) stator assembly; (b) conductors/slot diagram

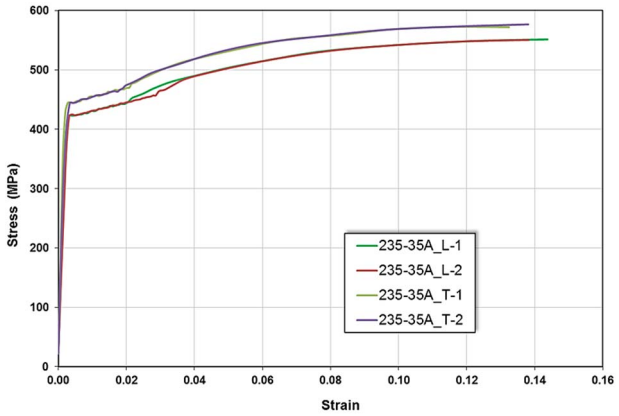

Fig. 3. Measured stress-strain for M235-35A

TABLE II MECHANICAL PROPERTIES CALCULATED FROM TENSILE TESTS (M235-35A)

Property	**Unit**	**Catalogue data**		**Experimental value**	
		TD*	**RD**	**RD**	**TD**
Yield strength R_{p02}	MPa	430	-	423-424	444-444
Ultimate strength R_m	MPa	450	-	551-550	572-577
Elongation A_{80}	%	18	-	-	-
Elongation A_{50}	%	-	-	20.5-21.6	23.6-22.7

* TD: Transversal Direction; RD: Radial Direction (longitudinal)

Fig. 2 shows the hairpin implementation for the inner rotor topology, with four conductors/slot. Such configuration allows the usage of one or two parallel path, depending on the available DC bus voltage level. Current technology allows a number of conductors/slot up to 8, but work is pursued to push this limit to 16. Note the requirement to use transposition of the coil segments to minimize the AC copper losses. That means, each path formed by series connected coils has to be placed in alternative slot layers along the motor periphery [13]

III. ELECTRICAL STEEL SELECTION

The specific materials suitable for the CR-IM design in traction applications, include electrical steels and copper alloys. Considering the rotational speed, it is possible to select optimum materials for the CR-IM from the mechanical point of view.

For the stator and rotor laminations, different silicon–iron (SiFe) and cobalt–iron (CoFe) alloys can be considered. CoFe ensures highest saturation magnetization, going above 2 Tesla, thus enabling highest power densities to be achieved. The actual value of saturation magnetization for CoFe depends on the annealing temperature, time of annealing, and annealing atmosphere; in general, the better the mechanical characteristics of the annealed material, the lower the saturation magnetization. However, even when annealed to the optimum mechanical properties, the saturation magnetization of CoFe is still significantly higher than SiFe (around 20% higher). Materials of CoFe type, are significantly more expensive compared with SiFe laminations, hence the material weight per kilowatt is intrinsically higher and is thus not considered for this project.

Another important parameter when choosing the lamination material for CR-IM is the amount of core losses generated in the lamination due to the relatively high fundamental (up to 1kHz) and switching frequencies (up to 20kHz). For a given frequency and flux density, the core losses are primarily influenced by the lamination thickness and the final annealing method. In general, the thinner the laminations, the lower the core losses. Electrical steels as thin as 0.1 mm with very low core losses, which are tailored specifically for high-frequency applications, are commercially available but again too expensive to CR-IM in EVs.

Four non-oriented electrical steel, silicon-iron type, have been considered for CR-IM. Tests on the steel samples have been performed:

a) Material 1: M235-35A (Non-Oriented, fully-processed, thickness 0.35 mm)
b) Material 2: M290-50JKE (Non-Oriented, semi-processed, thickness 0.50 mm)
c) Material 3: NO30-15 (Non-Oriented, fully-processed, thickness 0.30 mm)
d) Material 4: NO02-HS (Non-Oriented, fully-processed, thickness 0.20 mm)

The frequency values used in tests are: 50Hz, 400Hz, 800Hz, 1000Hz and induction levels were up to 1.8T; extrapolated to 2.1T in modelling.

Fig. 3 represents the stress-strain characteristics obtained in the transverse and longitudinal directions for two specimens of different lengths (L-1, L-2). The parts of the curves of interest, that is the linear parts, are very close to

each other, leading to similar mechanical properties in the two considered directions, as presented in Table II Also note that the measurements are in line with catalogue data.

The performance comparison when considering various electrical steel grades is given in Tables III (inner rotor) and Table IV (outer rotor)

TABLE III CR-IM INNER ROTOR PERFORMANCE WITH VARIOUS ELECTRICAL STEEL GRADES

Property	**Unit**	M235-35A	M290-50JKE	NO30-15	NO20-HS
Magnetizing Current at 50Hz	Arms	162	160	169	168
Magnetizing Current at 400Hz	Arms	157	152	156	155
Maximum Torque at 50Hz/400Hz	N.m	370/350	370/350	370/350	370/350
Maximum Core Loss/ Total Loss	kW	0.98/31	1.6/31	0.75/31	0.84/31

TABLE IV CR-IM OUTER ROTOR PERFORMANCE WITH VARIOUS ELECTRICAL STEEL GRADES

Property	**Unit**	M235-35A	M290-50JKE	NO30-15	NO20-HS
Magnetizing Current at 50Hz	Arms	170	170	170	170
Magnetizing Current at 400Hz	Arms	170	170	170	170
Maximum Torque at 50Hz/400Hz	N.m	350/320	350/320	350/320	350/320
Maximum Core Loss/ Total Loss	kW	3.15/29	7.2/31.5	2.5/25	2.4/27

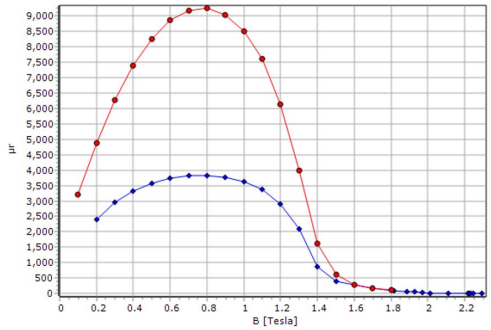

Fig. 4 Permeability vs Magnetic flux density – upper curve (red) published and lower curve (blue) experimental data, for M235-35A electric steel

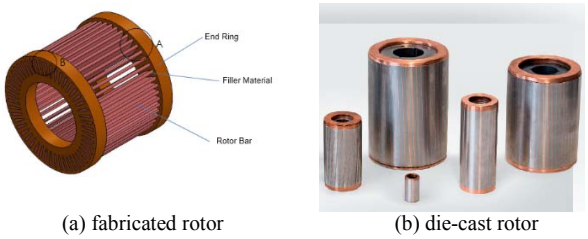

(a) fabricated rotor (b) die-cast rotor

Fig. 5. Illustrative for rotor cage assembly

M235-35A material was characterized at different frequency (50Hz, 400Hz, 800Hz, and 1000Hz) and induction levels, and using two cutting techniques: shear or lazer cutting. From this it was decided to use characterizations at 400Hz carried out on lazer cut laminations for further optimization. This choice is justified below:

- ***Frequency***. The frequency effect on performances was studied in D3.2. It was found that the torque at low speed was higher at 50Hz. As the machine operates at higher frequencies, characterizations at 400Hz were chosen.
- ***Cutting process.*** Generally speaking the punching process is cheaper. Also characterizations showed higher specific losses and lower permeabilities in case of lazer cut laminations. However, it is not economically justified to build punching devices that are intended for prototypes.

Fig. 4 shows the permeability vs magnetic flux density obtained from measured (red line) data at 50Hz and experimental (blue line) data at 400Hz. Here the differences are mainly due to the laser cutting process that induces thermal stresses in the laminations.

IV. COPPER ALLOYS SELECTION

Two options are considered for the rotor cage of CR-IM: die-casted and fabricated copper alloys. Fig. 5 illustrates the rotor cage assembly for CR-IM design [6], [7].

Table V shows the possible options for fabricated copper alloys and the methods that can be used to securely fixing the rotor bars to the end-rings: the industry standard is to solder them together; alternatively, the rotor bars can be welded to the rings. A copper-silver alloy (CuAg0.04) was selected, showing a good trade-off between electrical and mechanical properties. For die-cast rotor solution, alloy Cu-ETP was selected.

TABLE V. FABRICATED COPPER ROTOR MATERIALS

Characteristic	**Unit**	**Bars and end-rings**	**Filler**	
			Soldered	**Welded**
Material type	-	CuAg0.04	SAC305	Bercoweld K5
Tensile strength	MPa	338	29.7	220
Shear strength	MPa	-	27@20°C	17@20°C
Electrical resistivity	Ω.m ($\times 10^{-6}$)	1.702	10.4	5 - 6.67
Electrical conductivity	%IACS	101.3	16.6	25.8 - 34.4
Thermal conductivity	W/(m.K)	388	58.7	120 - 145

TABLE V. EQUIVALENT ROTOR RESISTANCE FOR VARIOUS COPPER ALLOYS

Copper cage type	**Material**	Referred rotor resistance @ 120°C [Ω]
Die-cast	Cu ETP	0.01973
Fabricated/ soldered end-ring	CuAg 0.04	0.0205
Fabricated/ welded end-ring	CuAg 0.04	0.01902

The difference between various solutions for the cage rotor material is related to the rotor equivalent resistance at 120°C. Table VI summarizes the values used in the electromagnetic analysis. Note the small variation in CR-IM performance when considering die-cast of fabricated copper alloys for the rotor cage.

V. DESIGNS SCALING

Scalability of electrical machines can be regarded in various aspects and approached based on the main criteria of the system operation.

For example, it is possible to maintain the machine topology, i.e. stator slots number and shape, rotor poles number and shapes, winding pattern, but modify the radial and axial dimensions with a given ratio. Consequently, the newly obtained design would share certain performance aspects as torque ripple or efficiency but will deliver different torque and power and will need different housing and fixture details.

For cost-effective solution in EVs traction application, it is desirable to retain the same dimensions and materials from one vehicle to another. One manufacturer would benefit from fitting a similar system motor-housing on a rear or front axle of different EVs, but achieving different power and torque levels with different power supply system (battery and inverter).

Keeping the same machine dimensions, materials, winding and housing has also another significant advantage for EVs industry: power can be controlled via different transmission gear ratio, while the peak torque at the vehicle axle does not suffer a reduction if the supply current is maintained the same ratio. For example, we can obtain a required total torque ($T_{vehicle}$) at the vehicle axle, with a gear ratio of 1:N or with 1:M, where the electrical motor will deliver a torque equal to $T_{vehicle}/N$ or $T_{vehicle}/M$. Obviously, the higher the gear ratio, the lower the required torque from the motor. Note that the total power will remain constant.

The selected designs for both inner and outer rotor configurations, can be scaled and used for various power levels, by just changing the power and control unit, as seen in Table VII and Table VIII. This means, that the same motor can be used as an electro-mechanical converter for power levels between 75kW and 200kW. An alternative option was investigated, i.e. using shorter axial length for the stator/rotor laminated packs. However, this solution is leading to significant lower peak torque and possibly suitable for vehicles with less demanding drive cycle.

We notice that the inner CR-IM must operate at higher speed, up to 18000-20000rpm, while outer CR-IM must operate at lower speed.

TABLE VII. SCALING RESULTS FOR INNER CR-IM

Rated peak power [kW]	Peak torque [Nm]	Maximum efficiency [%]	Maximum DC voltage [V]	RMS line current [Arms]	Maximum speed [krpm]
200	372	96	720	500	18 -22
75	192	95	350	275	13

TABLE VIII. SCALING RESULTS FOR OUTER CR-IM

Rated peak power [kW]	Peak torque [Nm]	Maximum efficiency [%]	Maximum DC voltage [V]	RMS line current [Arms]	Maximum speed [krpm]
200	353	94	720	500	15 - 18
75	157	94	350	250	10

This will require different gear ratio, but for inner CR-IM there are important advantages as: lighter and lower amount of materials, lower frequency: 4 poles @ 20,000rpm means 667Hz for inner CR-IM and 6 poles @ 15,000rpm means 750Hz for outer CR-IM.

VI. ELECTROMECHANICAL PERFORMANCE

The performance of both topologies, inner and outer rotor is investigated, considering:

- Maximum current = 500Arms
- Maximum speed = 20krpm (inner rotor); 15krpm (outer rotor)
- DC bus voltage = 720V
- Control strategy = Maximum torque/amp
- Motor temperature = 120^0C
- Loss components: DC and AC stator copper, rotor copper, stator/roto core, windage,stray load (Bearing loss is neglected at this stage of design)

Fig. 6 and 7 show the efficiency maps in motoring mode for inner and outer rotor topology respectively.

The electromagnetic performance analysis proves the better potential for inner rotor topology at higher speed operation, i.e. up and above 20,000rpm; while the outer rotor technology can be selected if the speed range operation is below 15,000rpm.

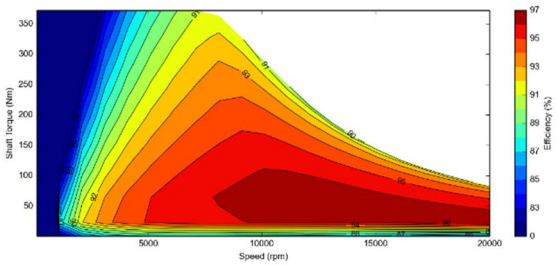

Fig. 6. Efficiency map for inner rotor CR-IM, with M235-35A steel

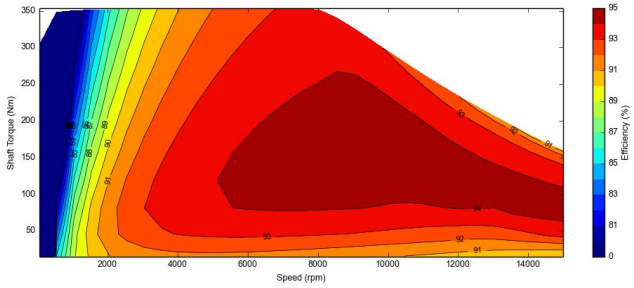

Fig. 7. Efficiency map for outer rotor CR-IM, with M235-35A steel

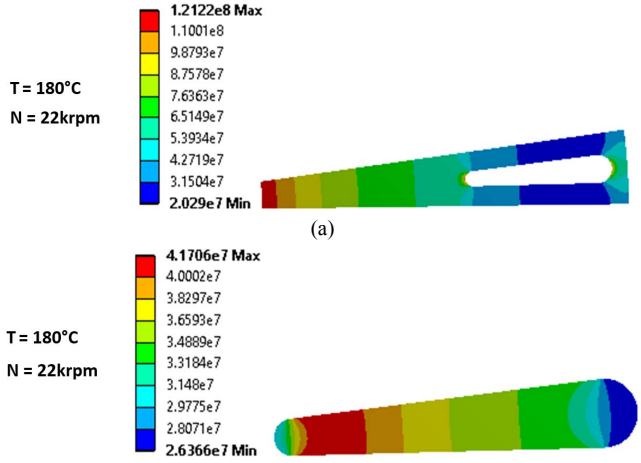

Fig. 8. Von Mises stress for inner rotor CR-IM, with (a) rotor core M235-35A steel and (b) copper bar (units in Pa)

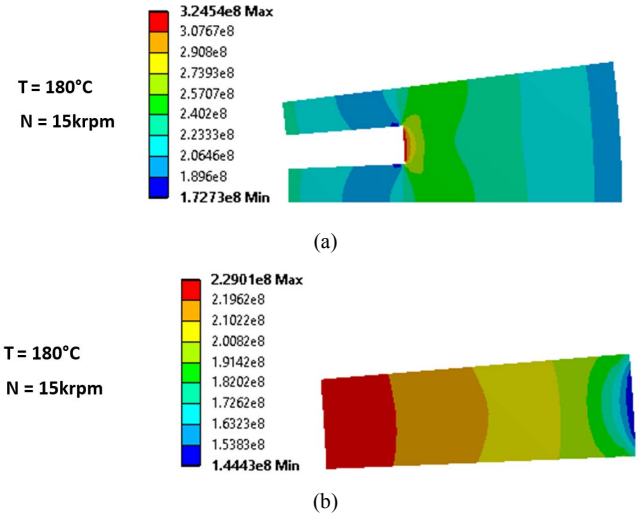

Fig. 9. Von Mises stress for outer rotor CR-IM, with (a) rotor core M235-35A steel and (b) copper bar (units in Pa)

If power density is main criteria in designing the power traction system, the inner rotor technology shows better potential.

The results for mechanical stress analysis performed at maximum speed and temperature for inner and outer rotor topologies are given in Figs. 8 and 9 respectively. Notice the limitations for outer rotor, where both the rotor lamination and rotor bar can be subjected to plastic deformation, i.e. Von Mises stress is close or higher than Yield stress. Therefore, the outer rotor configuration is decided not to be investigated further in section VII.

VII. Thermal Performance

In induction machines, most of the loss components are of electrical resistive Joule type and located in the stator winding and rotor cage. The iron losses may represent a more significant heat source only at higher speed operation. Also, the mechanical losses must be considered. From the temperature levels point of view, the critical points to be considered are described below.

Bearings. This motor components represents the most frequent cause of failure in IM. Bearings in motors are considered mechanical devices. However, they do possess electrical properties that affect their life time. Bearings are subject to currents that can cause significant damage if neglected. There are two classes of currents that can increase wear on the bearings. The first class is low frequency and the second class is high frequency.

For low frequency bearing currents, published experimental results showed that the shaft voltage threshold is approximately 300 – 500 mV. A solution to this type of bearing currents is to use insulated bearings, which will break the circuit path preventing the flow of the current. High frequency bearing currents occur when an inverter-fed controller is used because of the high dv/dt.

The following solutions to limit bearing currents are in place. These include:

- one or two insulated bearings
- hybrid or ceramic bearings
- filter on inverter to reduce/eliminate common mode voltage
- lower switching frequency
- insulated coupling between motor and load.

The rate of failure due to low or high frequency bearing currents is not known or not sufficient data is published for a correct assessment. Mechanical failure of bearings is known to lead to more than 50% of the overall electric motors failure. Motor bearings within an electric motor can be damaged from improper handling and storage, improper installation, misalignment, improper lubrication, start/stop processes, contamination, overhung loads and motor fan imbalance.

Contamination is one of the biggest reasons for bearing failure modes. This occurs when foreign contaminants or moisture enter the bearings, usually during the lubrication process. We can take steps to prevent contamination during the regreasing process to ensure that they are kept out.

It is also important that the motor is properly outfitted for the task for which it was selected. This means using the right bearings for its application. Motors that are using sheaves or sprockets that are mounted on the shaft will need roller bearings in the motor, which are common among most standard motors.

Lubrication can always be a major cause of failure because of the high temperature operation, when lubrication fluid loses its properties. Also, there are so many different places where one can improperly apply lubrication. Too much or too little lubrication, along with the improper form of lubrication, can lead to premature wear and tear. All motor greases should be polyurea-based, and not all purpose greases. One should always take the plug out of the bottom so that old grease can be drained properly. Also, release valves can help prevent over greasing.

Motor bearing seal failures tend to emerge from improper lubrication or installation. Own experience showed than improper lubrication can lead to more than 20% rate of failure for open field electric motors.

Other causes for the insulation failure are:

- Dirt: Dirt is one of the major sources that cause damage to the electric motors. It can damage the motor by blocking the cooling fan which causes its temperature to raise. It can also affect the insulating value of the winding insulation if it settles on the motor windings. Proper steps should be taken to prevent the motors from dirt. Shielding devices are available which are used for this purpose.
- Moisture: Moisture also affects the performance of electric motors. It greatly contributes in the corrosion of the motor shafts, bearings and rotors. This can lead to an insulation failure also. The motor inventory should be kept dry all the time.
- Vibration: There are a number of possible causes of vibration, such as misalignment of the motor. Corrosion of parts can also cause the motor to vibrate. The alignment of the motor should be checked to eliminate this problem.

Stator winding. This is limited by the insulation class, typically Class 180°C (H). Higher levels can be used by either using more expensive insulation classes, e.g. 220°C, 240°C or considering that each insulation class can withstand higher temperature levels than the standard, but with impact on the insulation life. Each 10°C temperature increase, leads to faster aging of the insulation, halving the life of a machine.

Winding insulation has a certain life and if subjected to overheating, the insulation can be aged rapidly. 55% of the insulation faults are due to the overheating. Therefore, a proper electromagnetic/thermal design of the motor is necessary and a proper insulation class selection.

Rotor cage. This has an indirect effect on the IM thermal response. Typically, a copper cage can operate safely at higher temperatures > 200°C. However, the high temperature will affect the rotor lamination insulation and can create circulating currents between lamination sheets. Also, the heat generated by the rotor cage losses will be extracted via conduction and propagated to the shaft and bearings.

For the thermal cooling system of IM, we consider twp possible solutions [7-11]):

(1) Housing Water Jacket (WJ) and shaft Spiral Groove (SG) cooling systems coupled in parallel, using Ethylene Water Glycole (EWG) mixture as a coolant. This type of cooling is used in the Tesla 60S and the Audi e-tron traction motors.

This cooling system was optimized with objective the continuous torque maximization at low speed. The variables include the housing thickness, the WJ channel dimensions (width and height), the shaft channel thickness and the flow rate distribution between the two flow paths. The main constraints regard the continuous power at maximum speed ($\geq$ 70kW) and the maximum pressure drop in the housing WJ ($\leq$ 10kPa). Table VIII provides the characteristics obtained from the optimization process. Note that the pressure drop in the shaft is not specified. This quantity depends on the turbulences between the two coaxial cylinders, namely the dimensions and speed of the rotor, and can only be calculated from extensive CFD analysis. However, the rotor dimensions are in line with existing technologies, so the cooling efficiency and manufacturability are guaranteed.

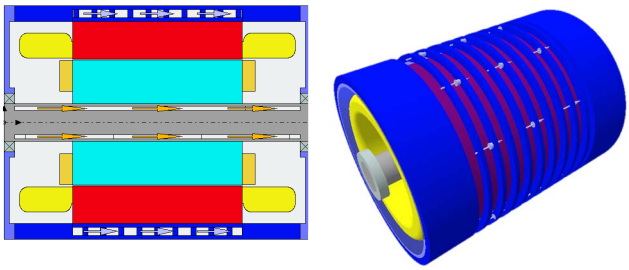

(a) Axial view (b) 3D view

Fig. 10. Cooling system (1)

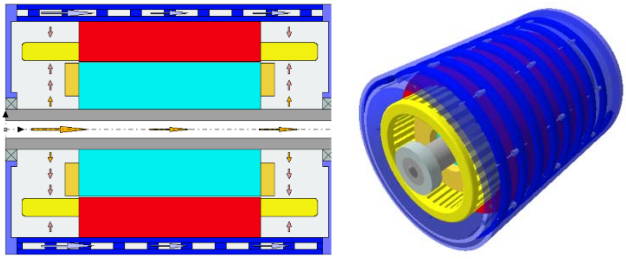

(a) Axial view (b) 3D view

Fig. 11. Cooling system (2)

TABLE VIII. MAIN CHARACTERISTICS OF COOLING SYSTEM (1)

Parameter	Unit	WJ	SG
Fluid inlet temperature	C	75	75
Fluid outlet temperature	C	83.38	79.26
Fluid flow rate	l/min	5.75	4.25
Pressure drop	kPa	10.42	-
Channel number	-	10	1

TABLE IX. MAIN CHARACTERISTICS OF COOLING SYSTEM (2)

Parameter	Unit	WJ	SG
Fluid inlet temperature	C	90	90
Fluid outlet temperature	C	6	2
Fluid flow rate	l/min	15	-
Pressure drop	kPa	10	1
Channel number	-	90	90

(2) Housing jacket and hollow shaft cooling systems coupled in parallel, with oil spray through nozzles placed on the shaft and the housing, using Automatic Transmission Fluid (ATF) as a coolant.

For comparison the second option with oil spray was designed using the same external envelope as the first cooling design. Its characteristics are given in Table IX. No optimization was performed in this case. Note that the pressure drop in the shaft is not specified. This quantity is very sensitive to the fluid velocity though the nozzles which varies with the rotational effects. Extensive CFD analysis are required for an accurate prediction. Alternatively, the nozzles dimensions were adjusted to limit the fluid velocity and the resulting pressure drop.

Figs. 10 and 11 show the axial and 3D geometry of cooling system (I) and system (II) respectively.

The machine's thermal behaviour was evaluated in transient operation for 30 seconds, without any potting material for end-windings. The estimated winding maximum temperature is 120^0C for cooling system (I) where a value of 195^0C was found for cooling system (II).

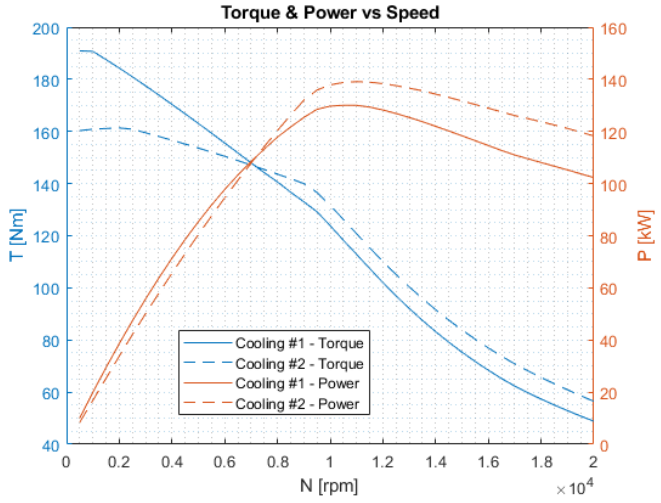

Fig. 12. Comparison between continous performance of cooling system #1 and #2

Fig. 12 shows the comparison between continuous performance of the inner rotor topology using the cooling systems. It was assumed that maximum acceptable temperatures are 180^0C for both the stator winding and rotor cage. Note the advantages of cooling system (1) at low speed, high torque operation, while cooling system is a preferred solution in case of operating points at high speed. The explanation for the latter, is given by the more efficient heat extraction of the AC copper losses in system (2) due to oil splash and spray technique.

VIII. Conclusions

The potential of induction machines in power traction systems for EV is investigated in this paper. Both inner and outer rotor topologies, with copper cage elements, show benefits.

Outer rotor configuration is limited due to mechanical stress values to lower speed (low gear ratio), when peak torque at low speed is the essential performance parameter. Inner rotor configuration represents a very good solution for higher speed, high power density solutions (high gear ratio).

The hairpin winding is a preferred technology for such application, due to the reduced DC copper loss and manufacturing suitable for automation.

Copper cages can be built using two technologies, die-cast and fabricated, with similar performance. The choice between modes of manufacturing the rotor cage depends on the production volume and investments.

The electrical steel grade is recommended to remain non-oriented, fully processed silicon iron, 0.35mm thickness, with possible grades: M235-35A, M250-35A, M270-35A or equivalent.

Dual cooling system with forced liquid convection for both the stator and rotor are necessary for any induction motor used in EV traction. Only one cooling system, be this on the stator or rotor assembly will lead to early thermal failure of either the bearings or stator winding respectively.

Acknowledgment

This work was funded under Horizon 2020, GV04 program, grant No. 770143.

The authors would like to acknowledge and thank their colleagues from RINA– Centro Sviluppo Materiali, Tecnomatic, Aurubis and Breuckmann for their contributions and useful discussions.

References

[1] Tesla Model S Pricing and Specs Revealed, MotorWard, 2011 [Online]. Available : http ://www.motorward.com/2011/12/tesla-model-s-pricing-and-specs-revealed/

[2] M. Burwell, J. Goss and M. Popescu "Performance/Cost Comparison of the Induction Motor and Permanent Magnet Motor in a Hybrid Electric Car" TechnoFrontier 2013, Tokyo, Japan

[3] R. Tiwari, Dr. A.K. Bhardwaj, "Analysis of Induction Motor with die-cast rotor". International Journal of Innovative Research in Electrical, Electronics, Instrumentation and Control Engineering, Vol 2, Issue 6

[4] Inside the HVH Hybrid Motor – Technical insights on Remy's "Off-the-Shelf" Hybrid Motor Solutions, White Paper, Remy Electric Motors, 2009

[5] D. Gerada et al, "High-speed electrical machines: Technologies, Trends and Developments", IEEE Transactions on Ind. Electronics., Vol. 61, No. 6, June 2014

[6] M. Caprio, V. Lelos, J. Herbst, S.Manifold, and H. Jordon, "High strength induction machine, rotor, rotor cage end ring and bar joint, rotor end ring, and related methods," U.S. Patent 7 504 756, Mar. 17, 2009.

[7] S. Jurkovic, K. Rahman, J. Morgante "Induction Machine Design and Analysis for General Motors e-Assist Electrification Technology", IEEE Transactions on Ind. App., Vol. 51, No. 1, Jan/Feb 2015

[8] M. Rosu, P. Zhou, D. Lin, D. Ionel, M. Popescu, F. Blaabjerg, V. Rallabandi, D. Staton *"Multiphysics Simulation by Design for Electrical Machines, Power Electronics and Drives"* , IEEE Press, Wiley 2018

[9] M. Popescu, D. A. Staton, A. Boglietti, A. Cavagnino, D. Hawkins and J. Goss, "Modern Heat Extraction Systems for Power Traction Machines—A Review" in IEEE Transactions on Industry Applications, vol. 52, no. 3, pp. 2167-2175, May-June 2016.

[10] S.H. Swales et al, "Oil cooled motor/generator for an automotive powertrain", US patent application #US 8169110 B2

[11] L. Fedoseyev and E.M. Pearce Jr."Rotor assembly with heat pipe cooling system", US patent application # 2014/0368064 A1

[12] G. C. Stone, I. Culbert, E. A. Boulter, H. Dhirani "Electrical Insulation for Rotating Machines: Design, Evaluation, Aging, Testing, and Repair", IEEE Press Series on Power Engineering, 2nd Edn. Wiley, 2014

[13] N. Bianchi, G. Beradi, "Analytical approach to design hairpin winding in high performance electric vehicle motors", IEEE ECCE, Portland, 2018, pp. 4398 - 4405